Author Manuscript

Author Manuscript

Author Manuscript

Author Manuscript

HHS Public Access

Author manuscript

Am J Undergrad Res. Author manuscript; available in PMC 2024 April 12.

Published in final edited form as:

Am J Undergrad Res. 2023 June ; 20(1): 77–84. doi:10.33697/ajur.2023.081.

Overexpression of *MMACHC* Prevents Craniofacial Phenotypes Caused by Knockdown of *znf143b*

Isaiah Perez,

Nayeli G. Reyes-Nava,

Briana E. Pinales,

Anita M. Quintana*

Department of Biological Sciences, University of Texas at El Paso, El Paso, TX

Abstract

ZNF143 is a sequence-specific DNA binding protein that regulates the expression of protein-coding genes and small RNA molecules. In humans, ZNF143 interacts with HCFC1, a transcriptional cofactor, to regulate the expression of downstream target genes, including *MMACHC*, which encodes an enzyme involved in cobalamin (*cbl*) metabolism. Mutations in *HCFC1* or *ZNF143* cause an inborn error of cobalamin metabolism characterized by abnormal *cbl* metabolism, intellectual disability, seizures, and mild to moderate craniofacial abnormalities. However, the mechanisms by which *ZNF143* mutations cause individual phenotypes are not completely understood. Defects in metabolism and craniofacial development are hypothesized to occur because of decreased expression of *MMACHC*. But recent results have called into question this mechanism as the cause for craniofacial development. Therefore, in the present study, we implemented a loss of function analysis to begin to uncover the function of ZNF143 in craniofacial development using the developing zebrafish. The knockdown of *znf143b*, one zebrafish ortholog of *ZNF143*, caused craniofacial phenotypes of varied severity, which included a shortened and cleaved Meckel's cartilage, partial loss of ceratobranchial arches, and a distorted ceratohyal. These phenotypes did not result from a defect in the number of total chondrocytes but were associated with a mild to moderate decrease in *mmachc* expression. Interestingly, expression of human MMACHC via endogenous transgene prevented the onset of craniofacial phenotypes associated with *znf143b* knockdown. Collectively, our data establishes that knockdown of *znf143b* causes craniofacial phenotypes that can be alleviated by increased expression of *MMACHC*.

*Mentor: aquintana8@utep.edu.

ABOUT STUDENT AUTHORS

Isaiah Perez earned a Bachelor of Science in Microbiology from the University of Texas at El Paso in December 2022. Currently, he is part of the Graduate Research Employee Program (GREP) working with Dr. Stephen C. Ekker and his research team at the Mayo Clinic. He will transition to the Mayo Clinic Graduate School of Biomedical Science to begin his graduate studies in the Regenerative Sciences Ph.D. program. His long-term goal is to become a principal investigator. For this project he was mentored by Dr. Quintana.

PRESS SUMMARY

ZNF143 interacts with HCFC1 to modulate the expression of downstream targets including MMACHC – an enzyme that binds to and processes cobalamin (or vitamin B12). Mutations in *HCFC1* or *ZNF143* cause an inborn error of cobalamin metabolism characterized by metabolic defects, intellectual disability, seizures, and mild to moderate craniofacial abnormalities. Although not a prevalent phenotype, the function of ZNF143 in craniofacial phenotypes is unknown. Here, we characterize the role of ZNF143 in facial development via a knockdown of *znf143b*, a zebrafish ortholog. Our study demonstrates that ZNF143 regulates craniofacial development which can partially prevented by over expression of MMACHC.

Author Manuscript Author Manuscript Author Manuscript Author Manuscript

Keywords

ZNF143; MMACHC; Vertebrate abnormalities; Cobalamin; *cblX*-like syndrome; Chondrocytes; Neural crest cells; Hyosymplectic

INTRODUCTION

Mutations in *ZNF143* have been associated with inborn errors of cobalamin (*Cbl*) metabolism. For instance, Pupavac and colleagues[1] reported mutations in *ZNF143* in a 16-month-old male patient with numerous clinical manifestations including methylmalonic acidemia and homocysteinemia which is indicative of *cbl* deficiency. Such manifestations are consistent with *cblX* (MIM 309541)[2] and *cblC* (MIM 609831) syndrome, two subtypes of *cbl* deficiency. Previous studies have demonstrated that mutation in *HCFC1* decrease expression of *MMACHC*, a downstream target gene whose mutation causes *cblC*. Interestingly, ZNF143 interacts with HCFC1 to regulate *MMACHC* expression.[3] This interaction occurs through binding of the ZNF143 DNA-binding domain (DBD) with the HCFC1 Kelch domain.[1,4] Consequently, mutations in either *HCFC1*, *ZNF143*, or *MMACHC* result in an inborn error of *Cbl* metabolism.

ZNF143 is a sequence-specific transcriptional activator that regulates protein-coding genes and small RNA molecules. In fact, two domains residing in the protein spur transcription selectively at either small RNA or mRNA promoters.[5] The phenotypes associated with mutations in ZNF143 in model systems have not been comprehensively studied, however, in zebrafish, loss of *znf143b* results in numerous abnormalities including defects in the heart, blood, ear, and midbrain hindbrain boundary.[6] Craniofacial phenotypes were not documented or characterized even though facial phenotypes have been observed across other subtypes of inborn errors of cobalamin metabolism[7]. Therefore, the focus of this study is to determine the effects of reduced *ZNF143* expression on facial development. Interestingly, zebrafish *znf143b* has a 71% overall amino acid sequence identity with the human protein. The conserved protein domains include the DBD, mRNA gene activation domain, and small RNA gene activation domain.[6]

HCFC1 encodes a transcriptional co-factor which lacks a DNA binding domain but interacts with transcription factors that include THAP11 and ZNF143.[8] Mutations in *HCFC1* result in a broad array of clinical manifestations including craniofacial abnormalities. In fact, knockdown of the zebrafish ortholog, *hcfc1b,* resulted in craniofacial abnormalities which are in part mediated by downregulation of *mmachc* expression.[3] Knockdown of *hcfc1b* caused an impairment in the differentiation of cranial neural crest cells (NCCs) which produce many facial cartilage structures. Given that mutations in *HCFC1* cause craniofacial defects via *mmachc* expression, it is likely that mutation or knockdown of HCFC1 interacting partners can also result in craniofacial abnormalities.[9] For instance, mutations in THAP11 have been associated with *cblX*-like manifestations including craniofacial abnormalities. Quintana and colleagues[9] have reported that knockdown of *thap11* causes defects in zebrafish facial development. Based on these data and the interaction between ZNF143 and HCFC1, we hypothesized that knockdown of *znf143b* will result in craniofacial

Author Manuscript Author Manuscript Author Manuscript Author Manuscript

abnormalities and downregulation of *mmachc*; consequently, assorting a mechanism by which *znf143b* regulates vertebrate facial development.

Here, we demonstrate that knockdown of *znf143b* results in abnormal craniofacial development in zebrafish. Morphant animals presented with an array of craniofacial defects which included a shortened and cleaved Meckel's cartilage, distortion of the ceratohyal, and a partial loss of ceratobranchial cartilages. In view of these defects, we analyzed chondrocytes, a derivative of NCCs, which contribute to cartilage formation. Flow cytometry found equal numbers of total chondrocytes in animals injected with *znf143b* MO and 3-dimensional rendering of chondrocytes did not indicate gross morphological defects. However, morphants had decreased expression of *mmachc* and cartilage phenotypes were effectively prevented using a human *MMACHC* transgenic allele. Collectively, these data suggest a function for *znf143b* in craniofacial development.

METHODS AND PROCEDURES

Zebrafish maintenance

Embryos were produced by crossing AB wild type, Tupfel Long Fin, *Tg(col2a1a:EGFP)*[10], or *Tg(ubi:MMACHC)*[11] adults. Fish were set up in a 2:3 or 2:2 ratio of females and males, respectively. Harvested zebrafish embryos were maintained in embryo medium at 28 °C. All animals were maintained and used in accordance with the guidelines from The University of Texas El Paso Institutional Animal Care and Use Committee protocol number 811869–5. Euthanasia and anesthetic procedures were performed according to the American Veterinary Medical Association guidelines, 2020 edition.

Morpholino injections

A validated antisense oligonucleotide morpholino (MO) was utilized to knockdown zebrafish *znf143b* expression (5' – GATCCATCCATTCATTCCATCAAT – 3').[6] Injections of MO and random control (RC) MO were performed at the single cell stage with a volume of 2 nL. A MO gradient from 0.20 mM (3.31 ng/embryo; N=34), 0.25 mM (4.14 ng/embryo; N=29), and 0.30 mM (4.97 ng/embryo; N=39) was performed. A final concentration of 0.30 mM was empirically derived, with an estimated 80% of morphant larvae affected at 5 days post fertilization (DPF). The injected embryos were incubated in E3 media at 28 °C and grown at 2- and 5- DPF for relative mRNA expression analysis and alcian blue staining, respectively. Morphant larvae were scored and allocated into groups based on the severity of craniofacial abnormalities ranging from mild, moderate, and severe. Morpholino injection was performed on 3 independent occasions with clutch mates obtained from independent carriers using equivalent numbers of total injected embryos/group. Carriers of *tg(ubi:MMACHC)* were mated and offspring were injected at the single cell stage with 0.30 mM of a translational blocking MO targeting *znf143b* or RC (GeneTools). Injected embryos were incubated at 28 °C and raised to 5 DPF for Alcian blue staining. Injection into the *tg(ubi:MMACHC)* was performed on two independent occasions with embryos obtained from independent male and female pairs with equivalent numbers of total injected embryos. Statistical analysis was performed using a Fisher's exact test between groups.

Author Manuscript Author Manuscript Author Manuscript Author Manuscript

Staining of cartilage and imaging

Zebrafish larvae were collected at 5 DPF and were fixed in 2% paraformaldehyde in PBS, pH 7.5 at room temperature for 1 hour. Larvae were washed for 10 min with 100mM Tris pH 7.5/10mM $MgCl_2$ and were stained overnight at room temperature with Alcian blue stain pH 7.5 (0.4% Alcian Blue in 70% EtOH, 1 M Tris pH 7.5, 1M $MgCl_2$). Subsequently, larvae were rehydrated in 80% ethanol, 50% ethanol, 25% ethanol in 100 mM Tris pH 7.5 for 5 minutes each. Larvae were bleached in 3% H_2O_2 and 0.5% KOH for 10 min at room temperature. Two washes with 25% glycerol/0.1% KOH were subsequently performed at room temperature for 10 minutes. All samples were stored at 4 °C in 50% glycerol/0.1% KOH. Larvae were whole mounted to visualize the viscerocranium at 6.3x magnification in 100% glycerol.

RNA isolation and quantitative PCR (qPCR) analysis

Total RNA was extracted with TRIzol reagent (Fisher Scientific) from a pool of whole-body embryos (n=10) injected with RC or *znf143b* MO at a concentration of 0.30 mM (4.97 ng/embryo) at 2 DPF. Analysis was performed in two biological replicates with embryos injected from independent clutches. cDNA was created using the Verso cDNA Synthesis kit (Fisher Scientific) and equivalent concentrations of total RNA were utilized. qPCR was performed in technical triplicate using a Sybr green (Fisher Scientific) based approach with primer pairs as follows: *mmachc* (FWD: GCTTCGAGGTTTACCCCTTCC, REV: AGGCCAGGGTAGGGTCCTG) and *rpl13* (FWD: TCCCAGCTGCTCTCAAGATT, REV: TTCTTGGAATAGCGCAGCTT). qPCR was performed with Applied Biosystems StepOne Plus system. Data analysis was performed using $2^{\Delta\Delta ct}$ and the statistics of relative mRNA expression was performed using a T-test ($p< 0.001$).

Chondrocyte image processing

Chondrocyte imaging was limited to visualizing the hyosymplectic region across all larvae at 5 DPF. Whole larvae were angled on the right ventrolateral angle and mounted with 0.6% low agarose gel in a glass bottom petri dish (Fisher Scientific). We obtained confocal imaging with Zeiss LSM 700 at 40X magnification. For all groups, 12 to 21 Z-slices were obtained per image. IMARIS software was employed to generate 3D visualization output. 3D renderings were produced from 10 individuals/group which include non-injected, random control, and morpholino injected. Fiji, an open-source platform, was utilized to calculate angles between individual chondrocytes in the hyosymplectic region. To ensure the angles were measured in a single plane, ImageJ software was used to apply a Fire LUT to provide a fluorescent intensity gradient with equal pixel measurements. The angle tool was used to draw the center of three adjacent cells along the region of interest. Length measurements of chondrocyte nuclei and the hyosymplectic were performed using the LUT and tools featured in Fiji. Measurements were performed in 5 technical replicates and the average angle across samples was used to test for statistical significance.

Flow cytometry

To enumerate chondrocytes, we utilized the *Tg(col2a1a:EGFP)* reporter line injected with a RC or *znf143b* morpholino at 0.30 mM. Whole larvae were dissociated by adapting a

Author Manuscript Author Manuscript Author Manuscript Author Manuscript

previous protocol from Bresciani and colleagues.[12] For each group, a pool of five larvae were dissociated using 500 μl of digestion mix (460 μl of 0.25% trypsin-EDTA and 40 μl of Type I Collagenase-100 mg/ml) at 30 °C. Larvae were fully homogenized via harsh pipetting. Dissociation was stopped by adding 800 μl of lamb serum (Fisher Scientific) and centrifuged (7.0 x g) for five minutes at room temperature. Cells were resuspended in 800 μl of 1X phosphate buffered saline (Fisher Scientific) and centrifuged for five minutes to wash the cells. Cells were resuspended in 500 μl of 1X phosphate buffered saline (PBS) and filtered (utilized 70 μM filter). Analysis was performed with Kaluza software at a fixed rate of 10,000 cell events for 3 minutes. A total of 10,000 events was collected per biological replicate (2 biological replicates were performed).

RESULTS

znf143b mediates craniofacial development and mmachc expression.

To perform a functional analysis of *ZNF143*, a transient knockdown of *znf143b* was performed. An antisense MO was previously designed to target the translation start site of *znf143b*, consequently, disrupting the translation of *znf143b* in zebrafish embryos. At 5 DPF, *znf143b* morphants were stained with Alcian blue to visualize the craniofacial development. Knockdown of *znf143b* resulted in a shortening of the Meckel's cartilage, partial loss of the ceratobranchial arches, and distortion of the ceratohyal (Figure 1A-D). Not all injected larvae replicated with the exact defects; however, roughly 84% (n = 16/19) of embryos injected with 0.30 mM of MO presented with abnormal craniofacial development (Figure 1F). All affected morphants (n=16) demonstrated with a shortened and cleaved Meckel's cartilage. We calculated that 16% (n = 3) of the total morphant embryos injected developed mild defects, while 21% (n = 4) had moderate defects. Interestingly, morphant animals with moderate defects developed heart edema in a similar fashion as those severely afflicted animals. The prevalence of a distorted ceratohyal was noted more in animals with severe defects. All morphant animals were categorized based on severity of structures shown in Table 1.

Pupavac and colleagues[1] reported reduced expression of *MMACHC* in a patient with a mutation in *ZNF143*. Mutations in *MMACHC* are known to cause a multiple congenital anomaly syndrome that is attributed to defects in cobalamin metabolism. Mild to moderate facial dysmorphia had been documented in patients with mutations in *MMACHC*.[13–15] In addition, mutations in *HCFC1* that cause *cblX* syndrome are also characterized with facial dysmorphia. Therefore, we hypothesized that ZNF143 interacts with HCFC1 to regulate the expression of *MMACHC*. As shown in Figure 1G, knockdown of *znf143b* caused a statistically significant 20% decrease in *mmachc* expression (p=0.0002).

Tg(ubi:MMACHC) expression prevents facial phenotypes in znf143b morphants.

Given the facial defects observed in morphant animals, we hypothesized that over expression of *MMACHC* could restore craniofacial deficits in *znf143b* morphants. The *Tg(ubi:MMACHC)* allele expresses the human *MMACHC* open reading frame under the control of the zebrafish ubiquitin promoter and was validated elsewhere.[11] We injected *znf143b* or RC morpholinos into the *Tg(ubi:MMACHC)* transgenic allele and stained them

Author Manuscript Author Manuscript Author Manuscript Author Manuscript

at 5 DPF with Alcian blue. Expression of MMACHC prevented the onset of *znf143b* mediated facial phenotypes (Figure 2C). As in the knockdown experiments, there was a statistical difference between animals injected *znf143b* and RC morpholinos (*p = 0.0248). The RC group had three mildly affected animals amongst a pool of twenty. In contrast, 19 of 23 morphant animals with wildtype background presented defects at 5 DPF (Figure 2B). Shown in Figure 2D, the total number of morphant animals in the mild, moderate, and severe groups was significantly reduced by expression of MMACHC, indicating that over expression MMACHC prevented the onset of facial phenotypes (**p = 0.0001).

znf143b does not exhibit abnormal chondrocyte stacking or defects in total cell number.

Knockdown of *znf143b* resulted in abnormal cartilage structures of the viscerocranium implicating a defect in neural crest cell (NCCs) developmental. Given the overt defects, we hypothesized abnormal development of chondrocytes, a derivate of NCCs that generate major skeletal structures of the viscerocranium. To test our hypothesis, we observed chondrocyte development in the hyosymplectic region using confocal microscopy and the *Tg(col2a1a:EGFP)* transgene. The hyosymplectic entails a region where the hyomandibula fuses with the symplectic rod and together secures the jaw skeleton to the neurocranium.[16] It is formed from pharyngeal arch 2[17], which also produces the ceratohyal. We observed the ceratohyal to be abnormally developed in morphant animals (Figure 1) and a recent publication from our laboratory demonstrated defects in chondrocyte development in a zebrafish mutant of *mmachc*.[11] For these reasons, we imaged the developing hyosymplectic using confocal microscopy. We rendered 3D visualizations using Z-slices from high resolution confocal microscopy (Figure 3A-C). We measured the angle of 3 adjacent nuclei as a measure of chondrocyte intercalation as previously described.[18] Angle measurements between three independent and adjacent chondrocytes was not statistically different between RC and morphant groups (p = 0.9621). Likewise, the length of the hyosymplectic was not significantly different between groups (p = 0.3064). We also sought to enumerate the total number of chondrocytes from whole larvae using flow cytometry. We did not detect a difference in the number of EGFP+ chondrocytes as shown in Figure D-D”(p=0.669818). These data suggest that knockdown of *znf143b* does not affect number or intercalation of chondrocytes.

DISCUSSION

A single clinical study has reported a biallelic pathogenic variant of *ZNF143* that causes a *cblX*-like syndrome.[1] The subject presented with increased levels of methylmalonic acid and homocysteine indicative of cobalamin deficiency. Additional phenotypes include intractable epilepsy, bilateral cleft palate, microcephaly, wide spaced eyes, progressive encephalopathy, and hypotonia.[1] These phenotypes are also observed in patients with *cblC* disorder which is caused by mutations in *MMACHC*.[19–20] However, mild and moderate facial defects[13–15] are not classic phenotypes associated with *cblC*. Interestingly, HCFC1 interacts with ZNF143 to modulate the expression of *MMACHC* and mutations in HCFC1 cause *cblX* syndrome, which is very similar phenotypically to *cblC*. Previous studies from Quintana and colleagues support a role for HCFC1 and MMACHC during zebrafish craniofacial development.[2,9] Similarly, our transient knockdown of *znf143b*, the zebrafish ortholog of

Author Manuscript Author Manuscript Author Manuscript Author Manuscript

ZNF143, caused reproducible craniofacial abnormalities in early zebrafish development. Interestingly, *znf143b* morpholino injected into embryos harboring an *MMACHC* transgene prevented morpholino induced craniofacial phenotypes. These data further support a role for *MMACHC* in facial development. [2,9,21] However the function of MMACHC in *cbl* disorders is likely to be more complex because NCC specific expression of MMACHC in a mouse model of *cblX* syndrome does not restore facial phenotypes.[21] These data suggest there may be some species-specific mechanisms at play as it relates to MMACHC function. Moreover, the function of MMACHC may not be autonomous to NCCs, and thus, a global expression strategy may be required to restore phenotypes present in HCFC1 and ZNF143 loss of function assays. Finally, HCFC1 and ZNF143 regulate an immense number of target genes[4] so it remains possible that *MMACHC* is not the sole genetic mediator of facial development in these *cbl* related disorders.

It is known that NCCs give rise to numerous tissues including chondrocytes of the viscerocranium.[22] Thus, it is plausible that the craniofacial abnormalities observed in our morphant larvae are caused by abnormal NCC development, specifically cranial NCCs. However, our limited analysis of chondrocyte development and chondrocyte number did not show abnormal organization or defects in the total number of chondrocytes. We only studied a single time point, a single NCC marker, and a single region of the developing viscerocranium. Morphants were affected in various cartilaginous elements. These include Meckel's cartilage and the ceratohyal, both of which were dramatically affected. Future studies that analyze these other regions with additional time points and/or additional markers of NCC development may uncover phenotypes in chondrocyte and NCC development.

ZNF143 is a ubiquitously expressed transcriptional activator [23] and is largely involved in cellular and molecular processes that include but are not limited to cell growth, proliferation, cell cycle regulation, DNA repair, and progenitor cell identity. [24–26] We therefore, analyzed the total number of chondrocytes using flow cytometry, which were normal. One possible explanation for the normal overall cell number we observed could be that although the expression of ZNF143 is ubiquitous, the function of ZNF143 is tissue specific. Thus, ZNF143 could regulate facial development independent of proliferation, cell number, or cell cycle regulation. Future studies should aim at studying alternative cellular mechanisms to elucidate the putative role of ZNF143 in NCC development. Alternatively, analysis of chondrocyte migration using live imaging could be performed. Previous studies have shown that migration is enhanced after knockdown of ZNF143 in colorectal cancer cells.[27]

Finally, mutation of ZNF143 causes accumulated levels of homocysteine and methylmalonic acid.[1] This biochemical manifestation was not explored in *znf143b* morphants. Some patients with cobalamin disorders present with facial phenotypes and abnormal biochemical levels. However, it is not known if the accumulation of metabolites contributes to craniofacial abnormalities. As of now, we know that knockdown of *hcfc1b*, a zebrafish ortholog of *HCFC1*, has no apparent changes in the levels of homocysteine and methylmalonic acid indicating normal metabolism of cobalamin.[2] Given its interaction with HCFC1, we can hypothesize that a knockdown of *znf143b* may show similar biochemical phenotypes in the zebrafish. Such a finding would implicate that craniofacial defects

Author Manuscript Author Manuscript Author Manuscript Author Manuscript

observed by knockdown of ZNF143 or HCFC1 are partially driven by MMACHC yet independent of cobalamin metabolism. Future work in this area is warranted.

CONCLUSION

In sum, our study functionally profiles the role of *ZNF143* in early craniofacial development using a zebrafish model. A morpholino mediated knockdown resulted in an array of craniofacial defects that include a shortened and cleaved Meckel's cartilage, distorted palatoquadrate and ceratohyal, and partial loss of the ceratobranchial cartilages. Alongside these apparent facial defects, we detected a decrease in the expression of *mmachc* mRNA. Injection of the *znf143b* MO into a transgenic allele overexpressing human *MMACHC* prevented the formation of craniofacial phenotypes suggesting some interplay between ZNF143 and MMACHC during craniofacial development. Further, we found no abnormal development of chondrocytes in the hyosymplectic region and normal levels of total chondrocytes.

ACKNOWLEDGMENTS

Financial Support for this project was provided by NIDCR grant number R03 DE029517 given to Dr. Anita M. Quintana, NIMHD grant No 5U54MD007592 to the University of Texas El Paso, NIGMS linked awards Rl5GM118969, TL4GM118971, and UL1GM118970 to the University of Texas at El Paso. The content is solely the responsibility of the authors and does not necessarily represent the official views of the National Institutes of Health. The authors thank UTEP Core facilities for providing instruments for flow cytometry and imaging analysis of chondrocytes and mRNA expression analysis.

REFERENCES

1. Pupavac M, Watkins D, Petrella F, Fahiminiya S, Janer A, Cheung W, Gingras AC, Pastinen T, Muenzer J, Majewski J, Shoubridge EA, Rosenblatt DS (2016) Inborn Error of Cobalamin Metabolism Associated with the Intracellular Accumulation of Transcobalamin-Bound Cobalamin and Mutations in ZNF143, Which Codes for a Transcriptional Activator, Hum Mutat 37, 976–982. 10.1002/humu.23037 [PubMed: 27349184]
2. Yu HC, Sloan JL, Scharer G, Brebner A, Quintana AM, Achilly NP, Manoli I, Coughlin CR 2ndGeiger EA, Schneck U, Watkins D, Suormala T, Van Hove JL, Fowler B, Baumgartner MR, Rosenblatt DS, Venditti CP, & Shaikh TH (2013) An X-linked cobalamin disorder caused by mutations in transcriptional coregulator HCFC1, Am J Hum Genet 93, 506–514. 10.1016/j.ajhg.2013.07.022 [PubMed: 24011988]
3. Quintana AM, Geiger EA, Achilly N, Rosenblatt DS, Maclean KN, Stabler SP, Artinger BK, Appel B, Shaikh TH (2014) Hcfc1b, a zebrafish ortholog of HCFC1, regulates craniofacial development by modulating mmachc expression, Dev Biol 396, 94–106. 10.1016/j.ydbio.2014.09.026 [PubMed: 25281006]
4. Michaud J, Praz V, James Faresse N, Jnbaptiste CK, Tyagi S, Schütz F, & Herr W. (2013) HCFC1 is a common component of active human CpG-island promoters and coincides with ZNF143, THAP11, YY1, and GABP transcription factor occupancy, Genome Res 23, 907–916. 10.1101/gr.150078.112 [PubMed: 23539139]
5. Huning L, & Kunkel GR (2020) Two paralogous znf143 genes in zebrafish encode transcriptional activator proteins with similar functions but expressed at different levels during early development, BMC Mol Cell Biol 21, 3. 10.1186/s12860-020-0247-7 [PubMed: 31969120]
6. Halbig KM, Lekven AC & Kunkel GR (2012) The transcriptional activator ZNF143 is essential for normal development in zebrafish, BMC Mol Biol 13, 3. 10.1186/1471-2199-13-3 [PubMed: 22268977]

Author Manuscript Author Manuscript Author Manuscript Author Manuscript

7. Cerone R, Schiaffino MC, Caruso U, Lupino S, & Gatti R. (1999) Minor facial anomalies in combined methylmalonic aciduria and homocystinuria due to a defect in cobalamin metabolism, J Inherit Metab 22, 247–250. 10.1023/a:1005521702298
8. Sloan JL, Carrillo N, Adams D, & Venditti CP (2008) Disorders of Intracellular Cobalamin Metabolism, In Adam MP (Eds.) et al., GeneReviews®. University of Washington, Seattle.
9. Quintana AM, Yu HC, Brebner A, Pupavac M, Geiger EA, Watson A, Castro VL, Cheung W, Chen SH, Watkins D, Pastinen T, Skovby F, Appel B, Rosenblatt DS, & Shaikh TH (2017) Mutations in THAP11 cause an inborn error of cobalamin metabolism and developmental abnormalities, Hum Mol Genet 26, 2838–2849. 10.1093/hmg/ddx157 [PubMed: 28449119]
10. Askary a., Mork L, Paul S, He X, Izuhara AK, Gopalakrishnan S, Ichida JK, McMahon AP, Dabizljevic S, Dale R, Mariani FV, Crump JG (2015) Iroquois Proteins Promote Skeletal Joint Formation by Maintaining Chondrocytes in an Immature State, Dev Cell 35, 358–365. 10.1016/j.devcel.2015.10.004 [PubMed: 26555055]
11. Paz D*, Pinales BE, Castellanos BS, Perez I, Gil CB, Jimenez-Madrigal L, Reyes-Nava NG, Castro VL, Sloan J,L, and Quintana AM (2023) Abnormal chondrocyte development in a zebrafish model of cblC syndrome restored by an MMACHC cobalamin binding mutant, Differentiation 131, 74–81. 10.1016/j.diff.2023.04.003 [PubMed: 37167860] * indicates equal contribution
12. Bresciani E, Broadbridge E, & Liu PP (2018) An efficient dissociation protocol for generation of single cell suspension from zebrafish embryos and larvae, MethodsX 5, 1287–1290. 10.1016/j.mex.2018.10.008 [PubMed: 30364607]
13. Biancheri R, Cerone R, Schiaffino MC, Caruso U, Veneselli E, Perrone MV, Rossi A, Gatti R. (2001) Cobalamin (Cbl) C/D deficiency: clinical, neurophysiological and neuroradiologic findings in 14 cases, Neuropediatrics 32, 14–22. 10.1055/s-2001-12217 [PubMed: 11315197]
14. Cerone R, Schiaffino MC, Caruso U, Lupino S, Gatti R. (1999) Minor facial anomalies in combined methylmalonic aciduria and homocystinuria due to a defect in cobalamin metabolism, J Inherit Metab Dis 22, 247–250. 10.1023/a:1005521702298 [PubMed: 10384379]
15. D'Alessandro G, Tagariello T, Piana G. (2010) Oral and craniofacial findings in a patient with methylmalonic aciduria and homocystinuria: review and a case report, Minerva Stomatol 59, 129–137. [PubMed: 20357739]
16. Mork L, & Crump G. (2015) Zebrafish Craniofacial Development: A Window into Early Patterning, Curr Top Dev Biol 115, 235–269. 10.106/bs.ctdb.2015.07.001 [PubMed: 26589928]
17. Birkholz DA, Olesnicky Killian EC, George KM, & Artinger KB (2009) prdm1a is necessary for posterior pharyngeal arch development in zebrafish, Dev Dyn 238, 2575–2587. 10.1002/dvdy.22090 [PubMed: 19777590]
18. Shull LC, Lencer ES, Kim HM, Goyama S, Kurokawa M, Costello JC, Jones K, Artinger KB (2022) PRDM paralogs antagonistically balance Wnt/β-catenin activity during craniofacial chondrocyte differentiation, Development 149, dev.200082. 10.1242/dev.200082
19. Lerner-Ellis JP, Tirone JC, Pawelek PD, Dore C, Atkinson JL, Watkins D, Morel CF, Fujiwara TM, Moras E, Hosack AR, Dunbar GV, Antonicka H, Forgetta V, Dobson CM, Leclerc D, Gravel RA, Shoubridge EA, Coulton JW, Lepage P, Rommens JM, Morgan K, Rosenblatt DS (2006) Identification of the gene responsible for methylmalonic aciduria and homocystinuria, cblC type, Nat Genet 38, 93–100. 10.1038/ng1683 [PubMed: 16311595]
20. Carrillo-Carrasco N, Chandler RJ, Venditti CP (2012) Combined methylmalonic acidemia and homocystinuria, cblC type. I. Clinical presentations, diagnosis, and management, J Inheri Metab Dis 35, 91–102. 10.1007/s10545-011-9364-y
21. Chern T, Achilleos A, Tong X, Hill MC, Saltzman AB, Reineke LC, Chaudhury A, Dsagupta SK, Redhead Y, Watkins D, Neilson JR, Thiagarajan P, Green JBA, Malovannaya A, Martin JF, Rosenblatt DS, & Poche RA (2022) Mutations in Hcfc1 and Ronin result in inborn error of cobalamin metabolism and ribosomopathy, Nat Commun 13, 134. 10.1038/s41467-021-27759-7 [PubMed: 35013307]
22. Suzuki T, Sakai D, Osumi N, Wada H, & Wakamastu Y. (2006) Sox genes regulate type 2 collagen expression in avian neural crest cells, Dev Growth Differ 48, 477–486. 10.1111/j.1440-169X.2006.00886.x [PubMed: 17026712]

Author Manuscript Author Manuscript Author Manuscript Author Manuscript

23. Huning L, & Kunkel GR (2021) The ubiquitous transcriptional protein ZNF143 activates a diversity of genes while assisting to organize chromatin structure, Gene 769, 145205. 10.1016/j.gene.2020.145205 [PubMed: 33031894]

24. Ye B, Shen W, Zhang C, Yu M, Ding X, Yin M, Wang Y, Guo X, Bai G, Lin K, Shi S, Li P, Zhang Y, Yu G, & Zhao Z. (2022) The role of ZNF143 overexpression in rat liver cell proliferation, BMC Genomics, 23, 483. 10.1186/s12864-022-08714-2 [PubMed: 35780101]

25. Izumi H, Wakasugi T, Shimajiri S, Tanimoto A, Sasaguri Y, Kashiwagi E, Yasuniwa Y, Akiyama M, Han B, Wu Y, Uchiumi T, Arao T, Nishio K, Yamazaki R, Kohno K. (2010) Role of ZNF143 in tumor growth through transcriptional regulation of DNA replication and cell-cycle-associated genes, Cancer Sci 101,2538–2545. 10.1111/j.1349-7006.2010.01725.x [PubMed: 20860770]

26. Ye B, Yang G, Li Y, Zhang C, Wang Q, & Yu G. (2020) ZNF143 in Chromatin Looping and Gene Regulation, Front Genet 11, 338. 10.3389/fgene.2020.00338 [PubMed: 32318100]

27. Paek AR, Lee CH, & You HJ (2014) A role of zinc-finger protein 143 or cancer cell migration and invasion through ZEB1 and E-cadherin in colon cancer cells, Molecular Carcinog 53 Suppl, E161–168. 10.1002/mc/22083

Author Manuscript Author Manuscript Author Manuscript Author Manuscript

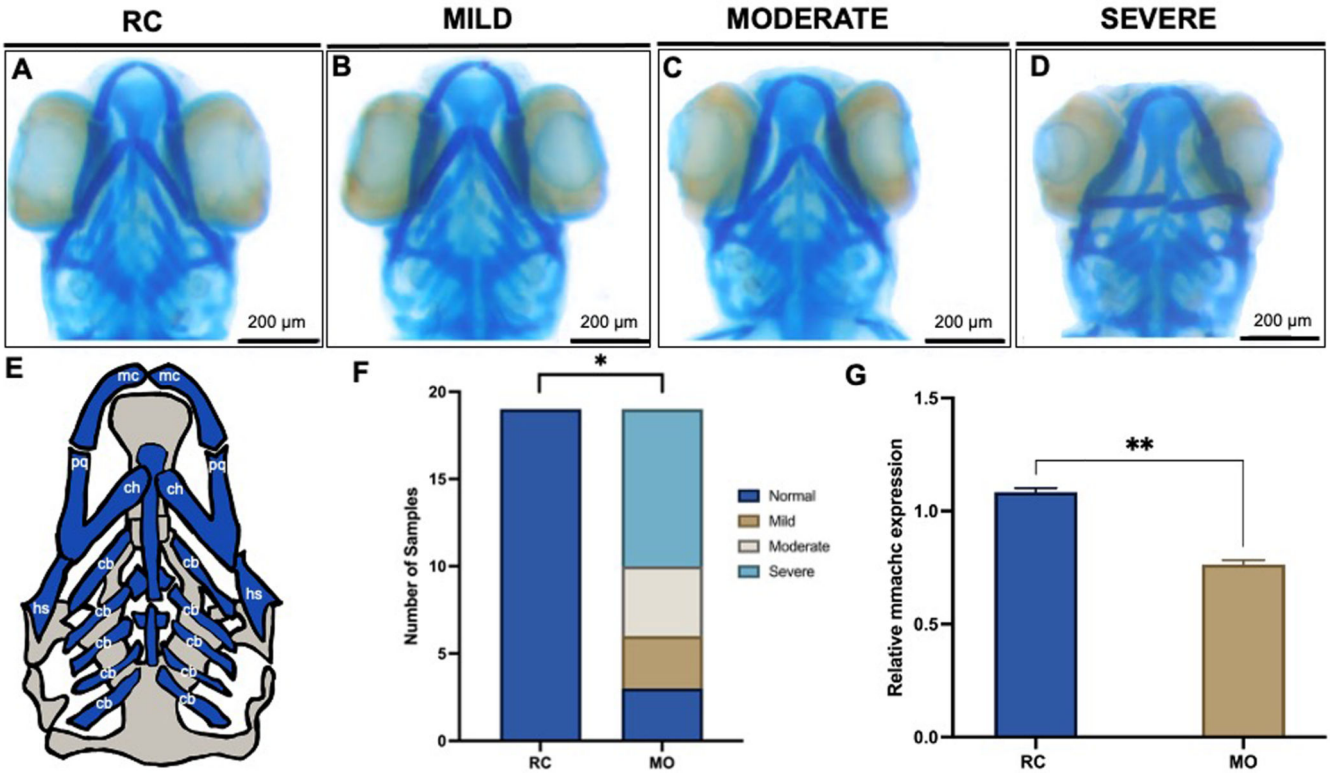

Figure 1.

Loss of *znf143b* causes a spectrum of craniofacial abnormalities and a decreased expression of *mmachc*. (A-F) Alcian-Blue stain reveals heterogeneous craniofacial defects at 5 days post-fertilization (DPF) in *znf143b* morphant larvae (MO) when compared to random control (RC) injected fish. E) Viscerocranium cartilage structures of zebrafish: Meckel's Cartilage (mc), Palatoquadrate (pq), Ceratohyal (ch), Certaobranchial arches (cb), and Hyosympletic (hs). F) Total number of RC (n=19) and MO (n=19) larvae categorized by craniofacial phenotypes. *Fisher's exact test* determined a significant difference between total number of affected and not affected animals (*p>0.0001) when comparing morphant (MO) and control injected (RC) larvae. Data represented here and the numbers of animals are a single representative of 3 biological replicates. G) Quantitative PCR demonstrated decreased expression of *mmachc* in *znf143b* morphants when compared to random control larvae (**p=0.0002). Representative experiment from 2 biological replicates is shown in (G).

Author Manuscript Author Manuscript Author Manuscript Author Manuscript

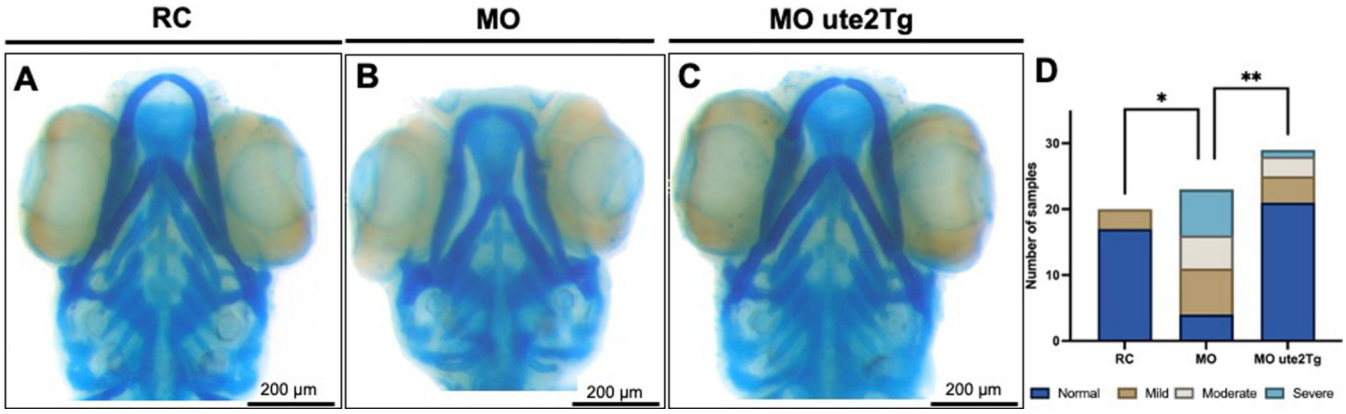

Figure 2.

Prevention of craniofacial defects upon expression of *MMACHC* in *znf143b* morphant larvae. (A-C) Representative images of alcian-blue stained random control (RC) and *znf143b* (MO) injected larvae, in wildtype and *Tg(ubiquitin:MMACHC)* (*ute2Tg*) background at 5 days post fertilization (DPF). (A) RC animals showed normal craniofacial features. (B) MO injected larvae exhibited abnormal craniofacial phenotypes (i.e. shorten Meckel's cartilage). (C) *znf143b* MO injection in animals with ubiquitous expression of *MMACHC (ute2tg)* prevented the craniofacial phenotypes induced by loss of *znf143b*. (D) Bar graph showing total number of RC (n=20), MO (n=23) and MO ute2Tg (n=29) larvae categorized by craniofacial phenotypes. Data represented here and the numbers of animals are a single representative of 2 biological replicates. Fisher's exact test determined a significant difference between RC: MO injected animals (*p=0.0248) and MO injected animals: MO ute2Tg larvae (**p=0.0001).

Author Manuscript Author Manuscript Author Manuscript Author Manuscript

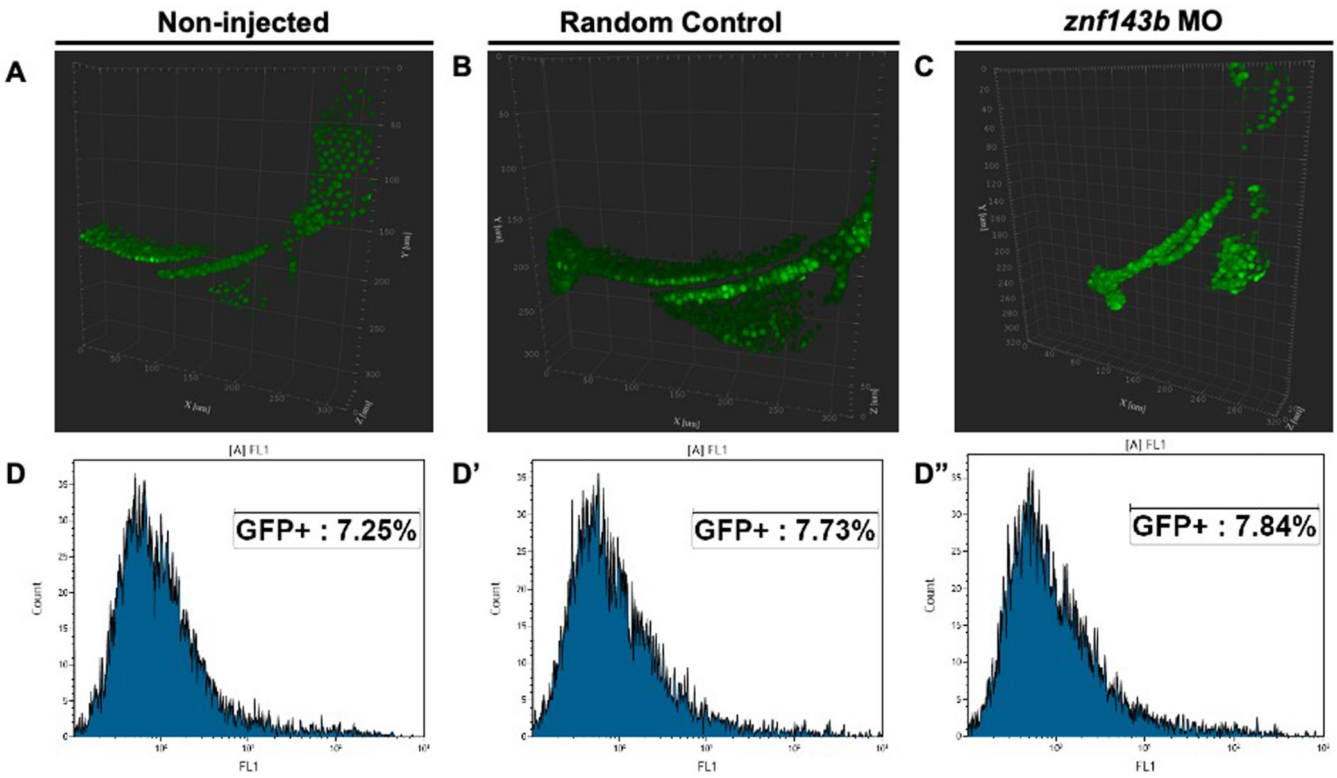

Figure 3.

Knockdown of *znf143b* does not affect chondrocyte development in the hyosymplectic region or total chondrocyte cell number. (A-C) Representative 3D visualizations of the hyosymplectic (HS) region of injected larvae harboring the *Tg(col2a1a:EGFP)* allele at 5 DPF. (A) Non-injected animals showed normal extension of the HS region. Normal chondrocyte development of the HS was observed in random control group (B) and *znf143b* MO injected animals (C). Standard T-test found no statistical difference between random control and *znf143b* MO injected groups regarding chondrocyte angle ($p = 0.9621$) and hyosymplectic length measurements ($p=0.3064$). We quantified the number of chondrocytes across all groups with the *Tg(col2a1a:EGFP)* using flow cytometry analysis. (D-D") Histograms of a single representative replicate displaying the percentage of GFP+ cells. Two biological replicates were performed 5 DPF from n=5 larvae/group. No statistical difference in the number of chondrocytes was found according to standard T-test ($p=0.669818$).

Author Manuscript

Author Manuscript

Author Manuscript

Author Manuscript

Table 1.

Phenotypic categorization of craniofacial defects observed in *znf143b* MO injected larvae.

Category	Phenotypes
Mild	Shorten/Cleave Meckel's Cartilage (MC)
Moderate	Shorten/Cleaved MC, torn palatoquadrate, distorted ceratohyal, heart edema
Severe	Shorten/Cleaved MC, loss of ceratobranchial arches, inverted ceratohyal, heart edema